INELASTIC BEHAVIOR OF STRUCTURAL COMPONENTS*

Noor Hussain, K. Khozeimeh and T. G. Toridis
School of Engineering and Applied Science
The George Washington University
Washington, DC 20052, USA

SUMMARY

The objective of this paper is to develop a more accurate procedure for the determination of the inelastic behavior of structural components. For this purpose, the actual stress-strain curve for the material of the structure is utilized to generate the force-deformation relationships for the structural elements, rather than using simplified models such as elastic-plastic, bilinear and trilinear approximations.

Force-deformation curves in the form of universal generalized stress-strain relationships are generated for beam elements with various types of cross sections. In the generation of these curves, stress or load reversals, kinematic hardening and hysteretic behavior are taken into account. Intersections between loading and unloading branches are determined through an iterative process.

Using the inelastic properties determined in this study, the plastic static response of some simple structural systems composed of beam elements is computed. Results are compared with known solutions, indicating a considerable improvement over response predictions obtained by means of simplified approximations used in previous investigations. The application of this procedure to the dynamic load case is currently in progress.

INTRODUCTION

Structural systems analyzed and designed for traditional loads and materials have been observed to undergo inelastic deformations when excessive load conditions are experienced. It is, therefore, an established fact now that inelastic deformations do occur in structures and are considered in the analysis in order to produce more economical and safe designs. For example, a generally accepted philosophy in the seismic analysis and design of structures is that a structure should remain elastic during earthquakes of small intensity that occur frequently; it should undergo limited plastic deformations during earthquakes of moderate intensity; however, it may undergo large plastic deformations but without major collapse during earthquakes of relatively high intensity that occur infrequently.

*This study has been partially supported by the National Science Foundation Research Grant No. PFR-79-16263.

At the same time, advances in naval, aerospace and nuclear reactor technology has led to the use of new materials such as stainless steel, alloys of aluminum and nickel, reinforced plastics, etc. The stress-strain curves for these materials are generally nonlinear. Therefore, an economical design of structures composed of such materials requires an accurate knowledge of the magnitude and distribution of the stresses and strains, as well as, the displacements. In all cases the effect of nonlinearities must be considered in the analysis.

In the study of the inelastic behavior of structures various idealizations to the actual stress-strain curves or force-deformation relations have been employed. The most extensively used model is the elastic perfectly plastic representation, principally due to its simplicity. When unloading occurs, this model neglects the strain hardening and Bauschinger effects. In general it produces conservative results and is mostly suitable for mild steel structures. Bilinear models with a nonzero slope for the inelastic branch have also been used widely. These models allow for the consideration of strain hardening effects (both isotropic and kinematic) due to loading and unloading cycles arising from static and dynamic loads. A trilinear model has also been used to simulate the stress-strain relationship of the material under static loads.

Simplified models often perform satisfactorily in predicting the inelastic behavior of special classes of structures. However, for general types of structures, an accurate representation of the stress-strain or force-deformation properties are needed for both the loading and unloading branches in the form of curvilinear or multilinear (piecewise linear) relations that follow as closely as possible the actual behavior of the system.

In the present study an accurate procedure is considered for the determination of the inelastic behavior of structural components. For this purpose, the actual stress-strain curve for the material of the structure is utilized to generate the force-deformation relationships for the structural elements, rather than using simplified models, such as elastic-plastic, bilinear and trilinear approximations. Applying this process to frame type structures, force-deformation curves in the form of universal generalized stress-strain relationships are generated for beam elements with various types of cross sections. In the generation of these curves stress or load reversals, more realistic strain hardening properties and hysteretic behavior are taken into account. Intersections between loading and unloading branches are determined through an iterative process. Based on the rather accurate force-deformation relationships of the individual elements, the governing equations for the structural system are established and used to compute the inelastic response of the structure.

GOVERNING EQUATIONS

Application of the Hamiltonian Principle to discrete systems in the context of the finite element method yields the basic dynamic equations governing the behavior of the structural systems. In matrix form these equations can be expressed as (ref. 1)

$$[m]\{\ddot{q}\} + ([K] + [K_G])\{q\} = \{F\} + \{F^O\} \tag{1}$$

where $[m]$ = consistent mass matrix of the structural system.

$[K]$ = elastic stiffness matrix of the structural system.

$[K_G]$ = geometric stiffness matrix of the structural system.

$\{q\}$ = vector of displacements at the structural degrees of freedom.

$\{\ddot{q}\}$ = vector of accelerations at the structural degrees of freedom.

$\{F\}$ = generalized nodal force vector corresponding to externally applied loads.

$\{F^O\}$ = equivalent generalized nodal force vector due to plastic strains, computed in accordance with the initial stiffness method.

In case of static loading the above equations take the form of

$$([K] + [K_G])\{q\} = \{F\} + \{F^O\} \tag{2}$$

PLASTICITY RELATIONS

Stress-Strain Curve

An experimentally determined virgin curve of the material is in general curvilinear. Starting with the experimental stress-strain data analytical expressions can be obtained to represent this data. Such expressions can be in the form of algebraic or other types of polynomials, exponential functions, or the widely used curvilinear relationship known as the Ramberg-Osgood approximation represented by

$$\varepsilon = \frac{\sigma}{E}\left[1 + D\left(\frac{\sigma}{\sigma_y}\right)^{R-1}\right] \tag{3}$$

in which ε and σ are the unit strain and unit stress, respectively, E represents the modulus of elasticity, σ_y denotes the yield stress of the material and D and R are real constants to be determined. However, this relationship is not explicit in stresses and, therefore, numerical procedures are needed to find the stresses corresponding to given strains. On the other hand, if the stress-strain data cannot be represented by an analytical expression, the curve is approximated by a series of line segments given by

$$\sigma = \sigma_i + k_{i+1}(\varepsilon - \varepsilon_i) \quad , \varepsilon_i < \varepsilon \leq \varepsilon_{i+1} \tag{4}$$

where, (σ_i,ε_i) are the stress-strain values at the beginning of the ith segment and k_{i+1} is the slope of the line segment between the points (σ_i,ε_i) and $(\sigma_{i+1},\varepsilon_{i+1})$ expressed as

$$k_{i+1} = \frac{\sigma_{i+1} - \sigma_i}{\varepsilon_{i+1} - \varepsilon_i} \quad , i = 0,1,2, \ldots, (n-1) \tag{5}$$

where n is total number of segments used to approximate the curve.

Moment-Curvature (Force-Deformation) Relationship

Figure 1 shows a general elasto-plastic doubly symmetric cross section of a beam member. A linear strain distribution over the depth of the cross section up to ultimate behavior is assumed. Tensile stresses are considered positive and curvatures causing positive strains at bottom fibers are also positive. The x- and y-axes are the principal axes and the z-axis is the geometric centroidal axis of the cross section. The bending moment acting on the cross section is the sum of moments of the stresses acting on the cross section about the geometric centroidal axis, i.e.

$$M = \int_A \sigma \, y dA \tag{6}$$

in which dA is an element of area. The integration is carried over the elastic and plastic parts of the area. Usually the stress-strain curve of the material cannot be represented explicitly for stresses; therefore, a numerical integration procedure is employed. For this purpose the section is divided into a series of rectangular slices, and the contribution of each slice to the moment acting over the cross section is found. Before indicating the details necessary for accomplishing this, certain definitions need to be established as follows. If ε_y, ε_u and σ_y are the yield strain, ultimate strain and yield stress, respectively, as observed in a tension test on a material and h is the distance to extreme fibers from z-axis, then

$$M_y = \sigma_y I_z/h = \sigma_y S \tag{7}$$

where M_y, I_z, S are the yield moment, moment of inertia and section modulus of the section, respectively. The yield curvature ϕ_y is obtained from

$$\phi_y = M_y/E I_z \tag{8}$$

Based on the assumption of a linear strain distribution over the cross section of the member, the ultimate curvature ϕ_u is given by

$$\phi_u = \varepsilon_u/h \tag{9}$$

In the present study the curvature range between ϕ_y and ϕ_u is divided into a suitable number of intervals to give enough data points to fit a curve. The strain ε_i at the center of ith rectangular slice, assumed to be uniformly distributed over the slice, corresponding to a curvature value ϕ_j is given by

$$\varepsilon_i = \phi_j y_i \tag{10}$$

where y_i is the distance to the centroid of the ith rectangular slice from the centroidal axis of the cross section. The strain ε_i in the ith slice due to curvature ϕ_j, at the jth discrete point along the member, is used to determine the stress σ_i assumed to act uniformly over the entire slice, from the stress-strain relationship as discussed previously. If A_i is the area of the ith slice, the force acting on the ith slice is given by

$$F_i = \sigma_i A_i \tag{11}$$

The moment of the force about the neutral axis is obtained from

$$M_i = F_i y_i \tag{12}$$

By summing over the total number of slices used to model the cross section, the total internal moment M_j on the cross section corresponding to a curvature ϕ_j is expressed as

$$M_j = \sum_{i=1}^{NS} M_i = \sum_{i=1}^{NS} \sigma_i A_i y_i \tag{13}$$

where NS is number of slices and j represents a typical discrete point along the member. Similarly the total internal axial force P at the cross section due to a prescribed strain field ε is obtained from

$$P = \sum_{i=1}^{NS} \sigma_i A_i \tag{14}$$

Equations (13) and (14) directly yield force P and moment M corresponding to a prescribed deformation field. However, to get the deformation corresponding to a given load history, equations (13) and (14) have to be solved iteratively. The moment curvature data generated through the use of equation (13) is then presented explicitly for curvature by a polynomial of the type

$$\phi = M/EI + \sum_{i=1}^{N} C_i M^i \tag{15}$$

where C_i are the polynomial coefficients to be determined and N is degree of the polynomial. Alternatively, an equation of the Ramberg-Osgood type

$$\phi = \frac{M}{EI}\left[\, 1 + D(M/My)^{R-1} \,\right] \tag{16}$$

can be fitted in which D and R are the real constants to be determined.

Normalized Moment Curvature Relationship

The moment-curvature data generated from Eq. (13) is normalized by using the quantities M_y and ϕ_y, so that

$$\bar{M} = M/M_y \tag{17}$$

$$\bar{\phi} = \phi/\phi_y \tag{18}$$

where $\bar{M}$ and $\bar{\phi}$ are normalized moment and normalized curvature, respectively. The normalized curvature is then separated into its elastic and plastic components $\bar{\phi}_e$ and $\bar{\phi}_p$, respectively, so that solving for $\bar{\phi}_p$

$$\bar{\phi}_p = \bar{\phi} - \bar{\phi}_e \tag{19}$$

Since $\phi_e = M/EI$, based on equation (17) the normalized elastic curvature is written in the form

$$\bar{\phi}_e = \bar{M} \tag{20}$$

Based on the normalized plastic components of curvature computed from equation (19), a polynomial of the form

$$\bar{\phi}_p = \sum_{i=0}^{N} d_i \bar{M}^i \tag{21}$$

is then fitted to approximate the data, where the d_i's are constants to be determined through regression analysis. Alternatively, an equation of the type

$$\phi_p = D\,\bar{M}^R \tag{22}$$

is also used to represent the data. The real constants D and R are determined by taking the logarithmic form of Eq. (22), so that

$$\ln \bar{\phi}_p = \ln D + R \ln \bar{M} \tag{23}$$

This is an equation of a straight line. Constants D and R are determined from linear regression analysis using the data for $\ln \bar{\phi}_p$ and $\ln \bar{M}$.

Using equations (19), (21), and (22), the following moment-curvature relations can now be formulated

$$\bar{\phi} = \bar{M} \qquad , \quad \bar{M} < 1 \tag{24}$$

$$\bar{\phi} = \bar{M} + \sum_{i=0}^{N} d_i \bar{M}^i \quad , \quad \bar{M} > 1 \tag{25}$$

$$\bar{\phi} = \bar{M} + A\,\bar{M}^R = \bar{M}\,[1 + A\bar{M}^{R-1}] \quad , \quad \bar{M} > 1 \tag{26}$$

Slope of Generalized Stress-Strain Curve

A universal stress-strain curve usually represents the relationship between $\bar{\phi}^P$ and $\bar{M}$ expressed by Eqs. (21) or (22). Rewriting these equations in differential form and solving for the slope $\bar{K}_2$ yields

$$\bar{K}_2 = \frac{d\bar{M}}{d\bar{\phi}^P} = \frac{1}{\sum_{i=1}^{N} i\, d_i\, \bar{M}^{(i-1)}} \tag{27}$$

and

$$\bar{K}_2 = \frac{d\bar{M}}{d\bar{\phi}P} = \frac{1}{AR\,\bar{M}^{(R-1)}} \tag{28}$$

If a smooth analytical expression to fit the $\bar{\phi}^P - \bar{M}$ data is not possible within tolerable limits of accuracy, the slope $\bar{K}_2$ of the universal stress-strain curve is obtained as a series of approximate tangents drawn at discrete points representing the data, i.e.

$$(\bar{K}_2)_i = \frac{\bar{M}_{i+1} - \bar{M}_i}{\bar{\phi}^p{}_{i+1} - \bar{\phi}^p{}_i} \tag{29}$$

where i and i+1 are typical discrete points.

In eqs. (21), (22) and (24)-(29) the cross section is assumed to be subjected to a bending moment about the centroidal axis. However, in practical cases, structural elements are generally subjected to stress resultants acting in different directions. To extend the applicability of the above procedure, it is assumed that similar relationships exist between the effective stress f* and effective strain Θ* in a multi-axial stress case. The function f* in normalized form is also identified with the yield function.

Yield Function

When stress resultants in normalized form (instead of unit stresses) are considered to be generalized stresses in the context of plasticity theory, yielding at any section of a member is then assumed to occur when the critical combination of generalized stresses initiate inelastic deformations at that section. The yield function is expressed by an equation of the form

$$f^*(Q_i) = Y \tag{30}$$

where Q_i are the generalized stresses and Y is the initial yield value. To make the yield function independent of the cross section, the yield function equation is derived in terms of normalized (dimensionless) force parameters. A force component is normalized by its corresponding characteristic value (usually the value at first yield). In normalized form equation (30) takes the form of

$$f^*(\bar{Q}_i) = 1 \tag{31}$$

For a space frame member the cross section is subjected to a generalized force vector S having 6 components, so that

$$\{S\} = \{P_x, V_y, V_z, M_x M_y, M_z\} \tag{32}$$

where

P_x = axial force

V_y, V_z = direct or transverse shear forces

M_x, M_y = Bending moments

M_z = Twisting or torsional moment

Each of these forces influence the yield behavior at a cross section and the inelastic response depends upon the interaction between them. In the past, elliptical, parabolic, spherical (ref. 2) and other forms of yield functions have been used in inelastic analysis of structures. In the present study a spherical yield function is used as indicated below

$$f^* = \left[\left(\frac{P_x}{P_{ox}} \right)^2 + \left(\frac{M_x}{M_{ox}} \right)^2 + \left(\frac{M_y}{M_{oy}} \right)^2 + \left(\frac{M_z}{M_{oz}} \right)^2 \right]^{\frac{1}{2}} = \bar{Y} \qquad (33)$$

in which $\bar{Y}$ denotes the normalized yield value which may change during straining and P_{ox}, M_{ox}, M_{oy} and M_{oz} are the characteristic values of axial force, torsional moment, and bending moments about y and z axes, respectively. Similar expressions can be written for a plate element (ref. 1).

The above yield function can be used in conjuction with an average force model (refs. 1, 3) which assumes that an element undergoes plastic deformations if the loading function f* determined from average values of stress resultants acting at the member ends exceeds the current normalized yield value.

Flow Rule

A flow rule expresses the relationship between plastic strains and stresses. In the present study rather than solving the flow equations rigorously in terms of stress resultants, an approximate procedure (refs. 1, 3) is employed. In this method if f^*_{est} is the plastic potential at the end of a load increment in dynamic analysis (computed using member forces $P_{i_{est}}$ obtained from an elastic analysis), then the increment of plastic potential df^*_1 for an element already undergoing inelastic deformation is obtained from the equation

$$df_1^* = f_{est}^* - f_{prev}^* \qquad (34)$$

where f^*_{prev} is the plastic potential at the end of previous load or time increment. For a transitional element the equation for the increment of plastic potential is of the form

$$df_1^* = f_{est}^* - f_o^* \qquad (35)$$

where f_o^* is the initial yield value.

As shown in detail in reference 1, the correct value of the plastic potential increment df* can be computed from the relation

$$df^* = \frac{\bar{K}_2}{1 + \bar{K}_2} \, df_1^* \tag{36}$$

The current corrected value of the plastic potential f^*_{curr} is then obtained as

$$f^*_{curr} = f_{prev} + df^* \tag{37}$$

for an element already undergoing plastic deformations and

$$f^*_{curr} = f^*_o + d_f* \tag{38}$$

for an element entering the plastic range.

With the known value of the plastic potential f^*, the final values of member (element) forces are computed by a proportioning procedure represented as (refs. 1, 3)

$$P_{i_{curr}} = P_{i_{est}} \frac{f^*_{curr}}{f^*_{est}} \tag{39}$$

The overall numerical procedure utilized in the computation of the element and structural responses is the same as the one outlined in references 1 and 2.

NUMERICAL RESULTS

To determine the feasibility of the proposed method, two structures for which results are available in the literature were analyzed and the results were compared with the works of other investigators.

Example 1 - The first example considered consists of the simply supported beam with the I cross-section and material property, as shown in figure 1. The given stress-strain curve corresponds to material B as defined by Chajes (ref. 4) who had originally studied this structure. As in the case of the above reference, the stress-strain curve is idealized by a bilinear relationship. This is then utilized to obtain the moment curvature and the normalized universal stress-strain curves, as depicted in figure 2.

Subsequently, the response of beam when subjected to either a concentrated load at its midspan or a uniformly distributed load over its entire length is obtained. It should be mentioned that Chajes (ref. 4) has presented a "closed-form" solution for the deformation characteristic of the midspan of the beam when subjected to a concentrated load. However, his solution is based on the assumption that only the flanges resist the bending moment. In figure 3 are shown the deflection responses of the midspan as obtained in this study as well as that reported in reference 4. As can be observed, close agreement between the two sets of data is exhibited.

Example 2 - As a second example, a pin-based portal frame studied, both theoretically and experimentally, by Takahashi and Chiu (ref. 5) is analyzed. The structure consists of W12X27 sections, arranged to deform around their strong axes. The geometry of the structure and its loading are shown in figure 4a. The idealized structure and the equivalent nodal loading is shown in figure 4b. Note that the effect of the girder depth has been taken into account by introduction of an additional equivalent load and a bending moment at the top of the loaded column. In the analysis, a curve is fitted to the stress-strain relation for the mild steel with an average yield stress of 255 MN/m^2 and modulus of elasticity of $203.5X10^3$ MN/m^2. This is then used as a basis for determination of moment-curvature relationship for the structure. In figure 4c is shown the horizontal deflection response of the top of the unloaded column. Again, close correlation is observed.

REFERENCES

1. Khozeimeh, K., "Inelastic Response of Beam-Plate Assemblages Subjected to Static and Dynamic Loads," dissertation presented to the George Washington University, at Washington, D.C., in 1974, in partial fulfillment of the requirements for the degree of Doctor of Science.

2. Morris, G. A., and Fenves, S. J., "Approximate Yield Surface Equations," Journal of the Engineering Mechanics Division, ASCE, Vol. 95, No. EM4, Proc. Paper 6741, Aug., 1969, pp. 937-959.

3. Khozeimeh, K., and Toridis, T.G., "Models for Inelastic Response of Beam-Plate Assemblages," Journal of the Engineering Mechanics Division, ASCE, Vol. 104, No. EM5, October 1978, pp. 1001-1014.

4. Chajes, A., "Inelastic Deflection of Beams," Journal of the Structural Division, ASCE, Vol. 94, No. ST6, Proc. Paper 6012, June, 1968, pp. 1549-66.

5. Takahashi, S. K., and Chiu, R. H., "Static and Dynamic Behavior of Pinned-Based Portal Frames," NCEL TR336, Feb., 1965.

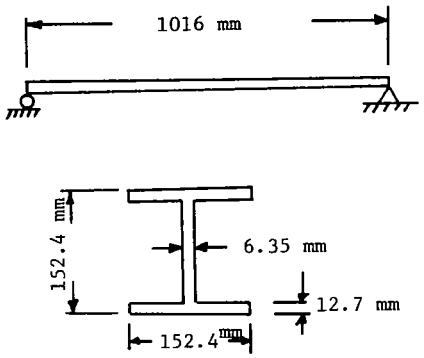

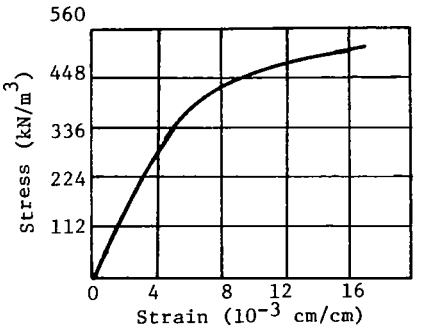

Figure 1.- Geometrical and material properties.

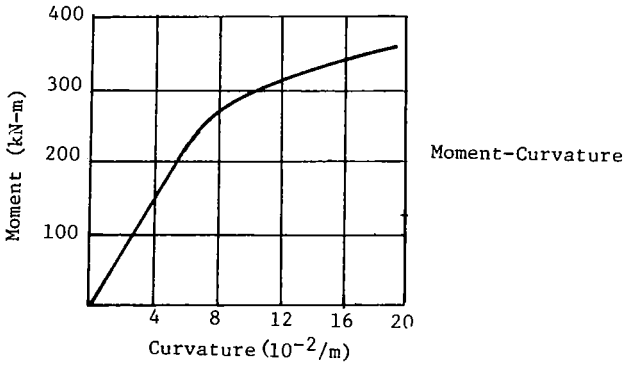

Moment-Curvature

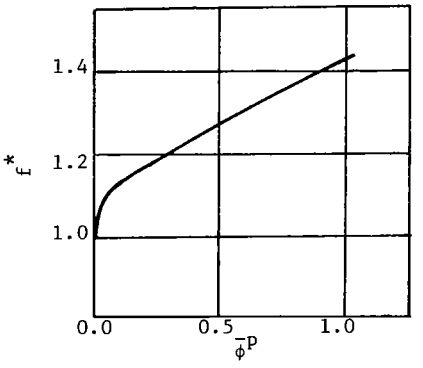

Universal Stress-Strain

Figure 2.- Moment-curvature and universal stress-strain curve.

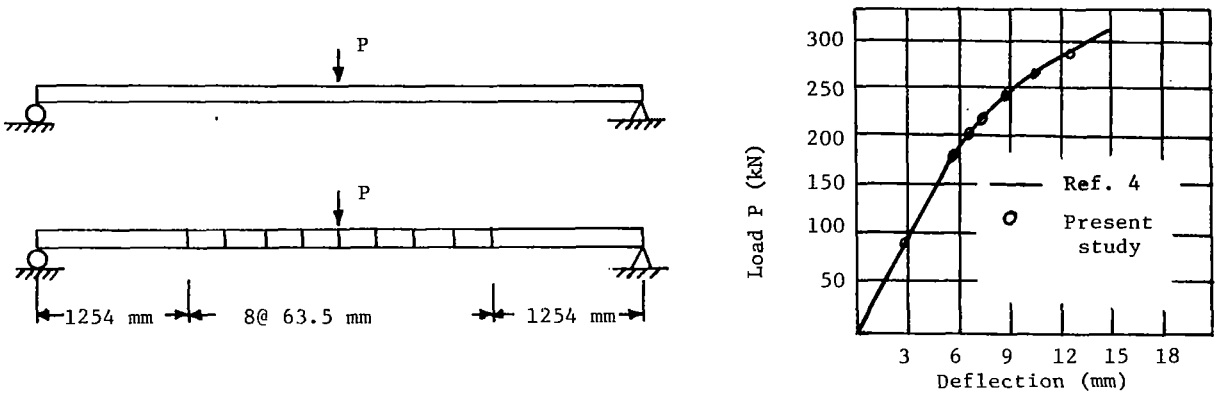

(a) Point load.

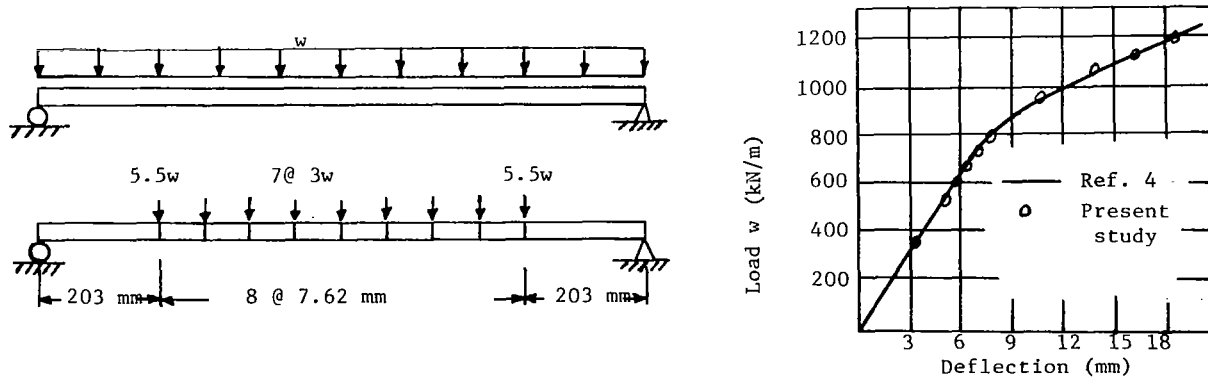

(b) Uniformly distributed load.

Figure 3.- Loading and mid-span deflection response.

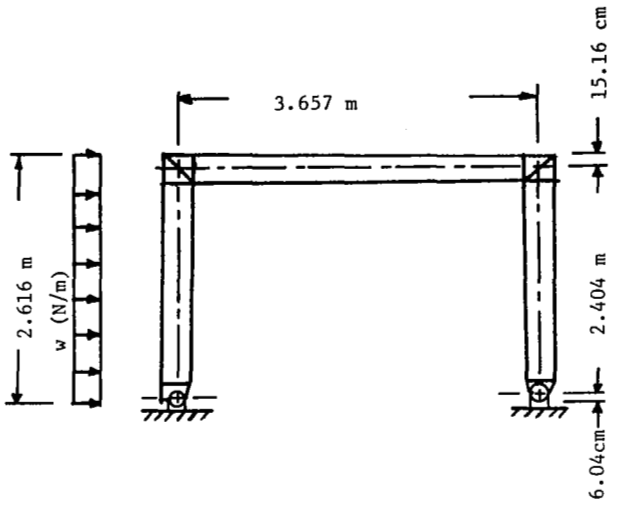

(a) Actual frame.

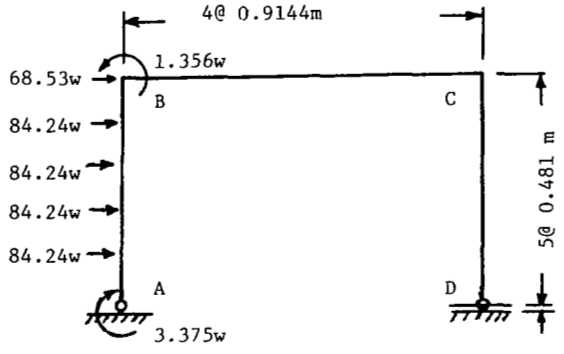

(b) Idealized frame.

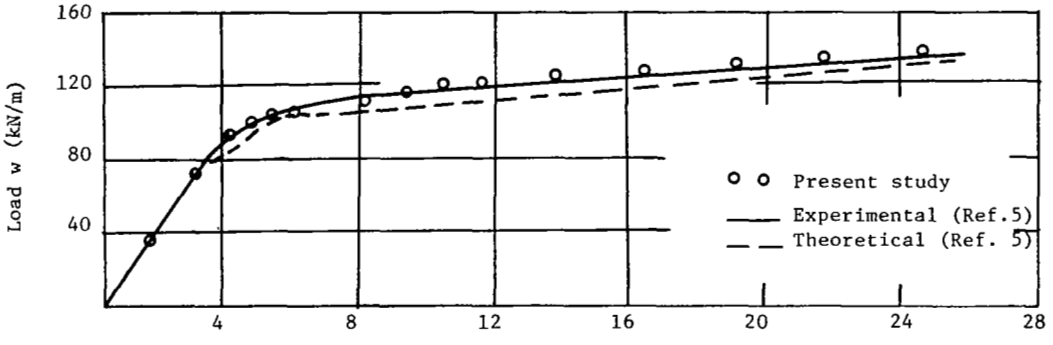

(c) Horizontal deflection of joint C (cm).

Figure 4.- Pin-based portal frame.